Bachelor Thesis

# Temperature dependence of the dielectric constant of oleic acid and its applications to biological membranes

Vardan Azizian
24/16/2014

Copenhagen University
Niels Bohr Institute
Membrane Biophysics Group

Supervisor:Thomas Heimburg

Co-supervisor: Karis Amata Zecchi

# Abstract

A parallel plate capacitor is used to measure capacitances at different temperatures and phases with oleic acid as a dielectric. The plate separation distance and temperature are controlled and the dimensions of the capacitor are known. With this setup, the dielectric constant of oleic acid is determined at different temperatures in solid and liquid phase, and during phase transition.

Biological membranes can be modelled as parallel plate capacitors and they undergo phase transitions at physiological temperatures. Thus a possible coupling of their dielectric and thermodynamic properties is of immediate relevance. With this motivation, the temperature dependence of the dielectric constant is experimentally investigated for oleic acid and the results are used as an exemplification of the fatty acid, hydrophobic cores of lipid membranes. The effect of electrostriction in biological membranes is discussed with respect to a temperature dependent dielectric constant.

Keywords: dielectric constant; lipid bilayer; oleic acid; electrostriction

**Table of Contents**

# 1. Introduction

All living creatures are composed of cells. All cells are enclosed by biological membranes and contain organelles, such as the endoplasmic reticulum, mitochondria which are also enclosed by membranes. Biological membranes are topologically closed physical barriers which, on a fundamental level, separate the interior of the cell from the exterior environment, just like the human skin separates atmosphere from flesh and bone. In the context of biomembranes, we are talking about membranes which are usually about 5 nm thick [1]. Other functions of the membrane in the cell are the transport and trafficking of chemicals entering and leaving the cell and their role as a medium for the propagation of electrical signals in the body i.e. action potentials.

Biological membranes are composed of lipids and proteins. Lipids are amphiphilic molecules which can spontaneously form a lipid double layer in aqueous environments such that the hydrocarbon chains align themselves opposite to one another and the head groups (if present, as in for example phospholipids – the most abundant species in biomembranes [2]) are in contact with the aqueous environments on either side of the membrane. This is energetically the most favourable arrangement since the hydrocarbon chains constitute the hydrophobic portion and the head groups constitute the hydrophilic portion of the lipids. As a result, the fatty acid hydrocarbon chains, which are sandwiched in between the two layers of head groups, function as a barrier with a very low dielectric constant $\varepsilon_r$~2-4, compared to that of water $\varepsilon_w \approx 80$. This physically means that a very high energy barrier must be overcome for any ions in the aqueous environment to cross this hydrophobic core [3].

A cell is the smallest physiological unit of independent life. Any living organism requires energy and a controlled traffic of chemicals going in and out. Therefore it is trivial that biomembranes are not completely impermeable and that small imperfections in the lipid bilayer of the membrane must be present to provide a selective permeability to specific ions which the cell might want to absorb or expel according to its needs. These imperfections either take the form of pores exclusively in the lipid portion of the membrane, whereby pores are formed in the membrane due to structural rearrangements of the lipids (e.g. anisotropies in the curvature) formed by mechanisms such as electroporation [4], lipid ion channels [5], or in the form of the embedded proteins, such as ion channels which can gate the flow of sodium ions, potassium ions and other chemicals across the membrane.

The flow of ions results in differences in concentrations of different ions in the solutions on either side of the membrane and therefore a net potential difference across the membrane called the transmembrane potential. Since we are dealing with an insulating layer between two charged (or conducting) layers, one can think of the biological membrane as a parallel plate capacitor. Just as a capacitor, the membrane is thought to have the role of storing and providing energy for a variety of 'molecular devices' embedded in the membrane. Its other function is to transmit electrical signals between different parts of the cell, particularly in electrically excitable cells such as neurons.

Another aspect of membranes is that they are an example of soft matter. This means that they can easily be deformed by any external stresses, including thermal fluctuations, near melting temperatures. Biological membranes display melting transitions between liquid and gel phase a few degrees below body temperature [6]. At phase transition temperatures, the

bulk properties of membranes are susceptible to small changes in temperature and they in turn can affect the electrical properties. Thus one can discover very interesting behaviours in membranes by simple relations of the various thermodynamic susceptibilities which would otherwise be impossible or very difficult to predict by studying single molecule interactions using more complex and experimentally unattainable mathematical models or computer simulations.. Since we are working with a system with infinite degrees of freedom, integrable models are also theoretically relevant.

Biophysics deals with *living* systems and in living systems there are always many physical processes occurring simultaneously. In the membranes of excitable cells, there are electrical signals being transmitted through action potentials and phase changes occurring in the constituent lipids – implying both mechanical and thermodynamic changes – all happening in the same system, at the same time. This poses the challenge of trying to isolate and identify the different processes taking place and subsequently determine whether a coupling can be predicted between them such that it can be experimentally tested. For example, in nerve axons, temperature changes, mechanical changes [6] [7], chemical changes and electrical changes [8] are all observed at the same time and the links are not completely clear, and more importantly it is unclear which one of these is the dominating process when signals are communicated along the axons.

With this motivation, in this project the dependence of relative permittivity on temperature for fatty acids and its implications to biological membranes are discussed. In particular, the relative electrical permittivity of oleic acid is related to temperature. Oleic acid is one of the fatty acids which are abundant in natural vegetable oils such as canola and olive oil. Since membrane phospholipids usually have one or two fatty acid chains (the hydrophobic part), bulk properties of oleic acid can serve as a model for those of the fatty acid cores in the lipid bilayer of membranes. Since membranes are capacitors and at the same time systems which have thermal fluctuations and phase changes at physiological temperatures, it is interesting to investigate if the bulk dielectric properties of the membranes change with temperature or with phase.

Even though the relative dielectric constants of oils are low, any significant change with temperature would directly affect the capacitive behaviour of the membrane, which could in turn produce additional mechanical forces on the membrane in electromechanical processes such as electrostriction [9] and piezoelectricity [9], or flexoelectricity [10].

The theoretical implications of such dependence are discussed with emphasis on membrane electrostriction and a specifically designed experimental setup is described and used to directly measure the capacitance across a parallel plate capacitor at different temperatures, with oleic acid as the dielectric medium between the plates. From this data, the bulk static dielectric constant is calculated.

In the following, a theoretical background is provided with an introduction to the structure of a biological membrane as it is currently known, the thermodynamic and electric properties of lipid membranes are introduced, electrostriction is introduced and finally the chemical structure of oleic acid is described. Subsequently, the materials, methods and original plan of the experiment are given with some of the problems and their solutions

encountered during experimentation. Finally, the results are given and analysed, followed by a discussion and outlook of the investigation.

# 2. Theoretical Background

## 2.1 Membrane Structure

### 2.1.1 Historical perspective

Biological membranes are macroscopic ensembles of mostly lipids and proteins. Lipids self-assemble into a 5-8 nm thick lipid bilayer in aqueous environments. The first evidence of this was given by Gorter and Grendel in 1925 [11], when they discovered that the surface area of lipids extracted from red blood cells was double the surface area of the cells. The conclusion was that the cell membrane must contain two layers of lipids. In 1935, Danielli and Davson revised this to include proteins in the membrane [12]. This model was revised and optimised into the popular 'fluid mosaic model' given by Singer and Nicolson in 1972 [13], shown in Figure 1 (left). Here the peripheral proteins and integral proteins are respectively absorbed to or span through the lipid matrix. In 1984, this was further refined by Mouritsen and Bloom into the 'mattress model', which allowed for inhomogeneous distributions of both lipids and proteins and the formation of clusters and domains [14] (Figure 1 -right). In this model, proteins and lipids interact with a positive free energy as the hydrophobic tails of the lipids vary. The modern picture of the biomembrane also includes lateral heterogeneities, and cluster and domain formations in the membrane [15] (Figure 2).

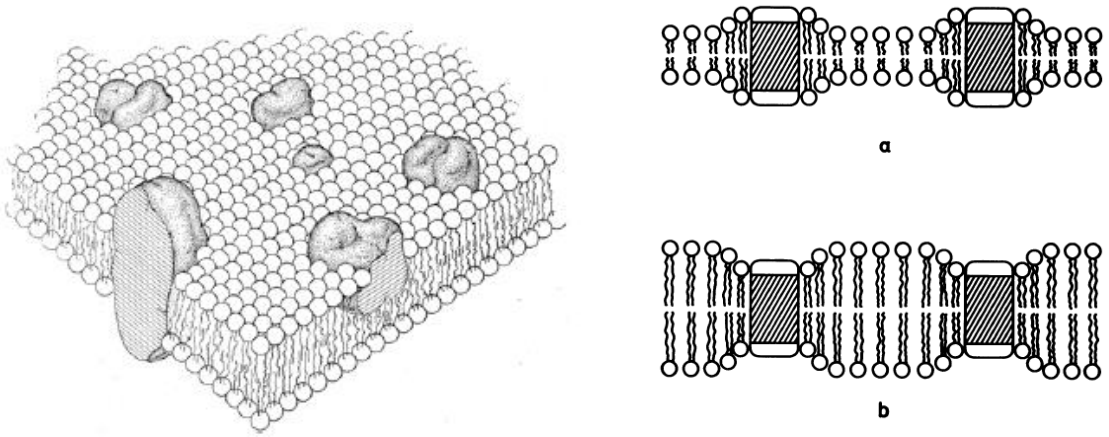


**Figure 1** ***Left:*** The 'fluid mosaic model' of Singer and Nicolson. The lipid bilayer is seen with both peripheral and transmembrane proteins embedded with a nonhomogeneous distribution **[13]**. ***Right***:The Mattress Model. The cross section of two lipid bilayers are shown and their interactions with rod shaped transmembrane proteins which are a) longer than the lipids and b) shorter than the lipids. **[14]**

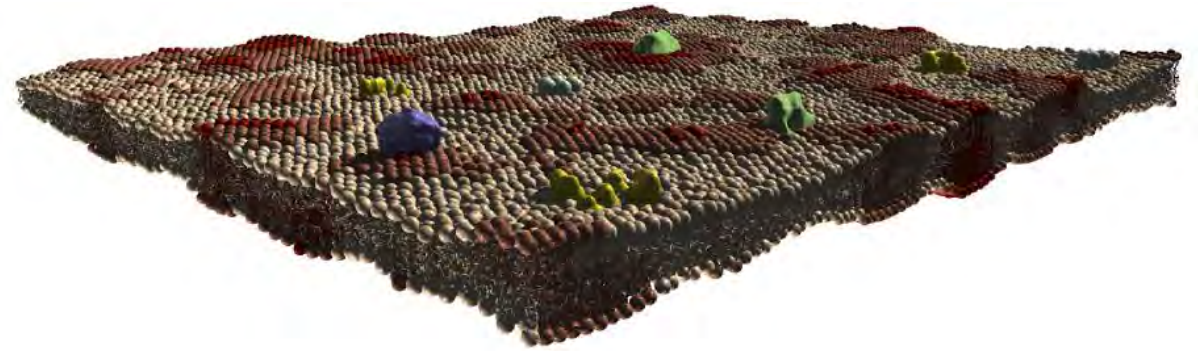

**Figure 2** Modern picture of the membrane **[2]**. Non-homogeneously distributed peripheral and transmembrane proteins are shown, with clusters, lipid protein interactions and lateral inhomogeneities.

The membrane surface area is mostly dominated by lipids [14], so any research concerning a pure lipid bilayer or lipids has an immediate relevance to real biological membranes.

Because membranes are elastic, anisotropic systems, they can be compared to and modelled by liquid crystals – states which are intermediate between crystalline solid and amorphous liquid [16].

### 2.1.2 Phospholipids

A class of amphiphilic lipids known as phospholipids are the most abundant in membranes [17]. They are composed of a hydrophilic head group, consisting of a negatively charged phosphate group and an organic molecule (e.g. a choline group), and a hydrophobic diglyceride tail. A common example of a phospholipid encountered in membranes is the DPPC molecule (1,2-Dipalmitoyl-sn-Glycero-3-Phosphocholine). The schematic drawing of DPPC is given below.

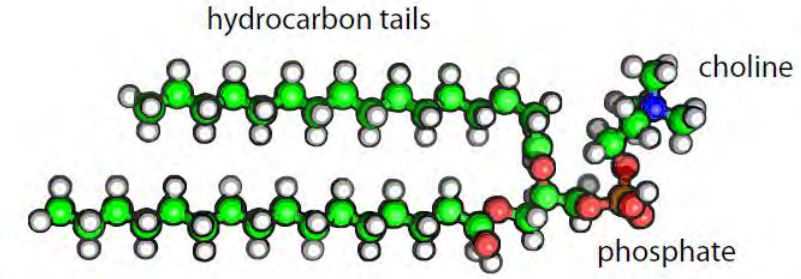


**Figure 3** The structure of a DPPC molecule. The three parts of a phospholipid are clearly shown; the hydrophobic tails, and the head group consisting of a phosphate and a choline group. **[2]**

The head groups may be negatively charged or neutrally zwitterionic, and may vary in size, and polarity, depending on the type of molecule which is attached to the phosphate group. These properties can affect the electrical properties of the membrane and its binding properties with proteins or drugs.

The hydrophobic tails are hydrocarbons which can be of various lengths and can display structural differences such as gauche and trans isomerisms, as well as double bonds (unsaturated chains).

## 2.2 Thermodynamic Properties of Lipid Membranes

We are interested in the effect of a temperature dependent dielectric constant on the melting of a biological membrane. In that respect, some fundamental thermodynamics is introduced in the following with emphasis on susceptibilities and phase transitions.

### 2.2.1 Laws of Thermodynamics

The first law of thermodynamics is the law of conservation of energy:

$$dE = \delta Q + \delta W \tag{1}$$

where $dE$ is the change in internal energy of a system and is a function of state. A function of state is function which describes the state of a system, independently of how it arrived there. Mathematically, this means that its value should be independent of the path taken to achieve it and the closed path integral is zero. $\delta Q$ and $\delta W$ represent infinitesimal changes in heat absorbed by the system and work performed on the system, respectively. The work performed on the system can be represented as the sum of all the different types of work which can be performed, represented by the product of an intensive variable $\mu_i$ (a variable which is independent of the size of the system) by the change in its conjugate extensive variable $dn_i$ (a variable which changes with the size of the system):

$$\delta W = \sum_i \mu_i dn_i \, \delta W \tag{2}$$

Examples of work performed on a biological membrane are:

- $-pdV$ – the work required to change the volume, where $p$ is the bulk pressure and $-dV$ is the change in volume
- $-\Pi dA$ – the work required to change the area, with membrane area $A$, and lateral pressure $\Pi$
- $-fdl$ – the work required to change the length of a spring, with the force $f$ and distance $l$
- $\Psi dq$ – work performed to charge a capacitor, with $\Psi$ as the electrostatic potential and $dq$, the change in charge on the membrane
- $EdP$ – work done to polarise the membrane, with $E$ the electric field, $P$, the change in net polarisation

Other functions of state are:

$$\mathrm{F} = \mathrm{E} - \mathrm{TS} \tag{3}$$

$$\mathrm{H} = \mathrm{E} + \mathrm{PV} \tag{4}$$

$$G = E + pV - TS \tag{5}$$

which are the Helmholtz free energy, the enthalpy, and the Gibbs free energy, respectively.

One way of formulating the second law of thermodynamics is:

$$dS = dS_r + dS_i \geq \frac{dQ}{T}, \quad \text{where } dS_r = \frac{dQ}{T} \text{ and } dS_i \geq 0 \tag{6}$$

where $S$ is the total entropy of the system, $S_r$ is the entropic contribution of the reversible processes, $S_i$ is the entropic contribution of irreversible processes, $dQ$ is the heat absorbed by the system, and $T$ is temperature. Entropy is also a function of state and it relates the heat changes of the system to the temperature. In the context of membrane melting transitions, the entropy of irreversible processes can be disregarded, since phase change is a fully reversible process.

So $dQ = TdS_r$ and substituting this into the first law yields:

$$dE = TdS_r - pdV - \Pi dA + \Psi dq + EdP + \cdots + \mu_n dn_n \tag{7}$$

The intensive variables can be expressed as the partial derivative of the internal energy with respect to their conjugate extensive variables, where the remaining variables are kept constant. Examples:

$$T = \left(\frac{\partial E}{\partial S_r}\right)_{V,A,q,\ldots} \tag{8}$$

$$p = -\left(\frac{\partial E}{\partial V}\right)_{S_r,A,\ldots} \tag{9}$$

$$E = \left(\frac{dE}{dP}\right)_{S_r,V,\ldots} \tag{10}$$

Alternatively, the second law can be expressed in terms of the sum of products of thermodynamic forces ($1/T$, $p/T$,…) and the change in their conjugated coordinates:

$$dS = \frac{dE}{T} + \frac{p}{T}dV + \frac{\Pi}{T}dA - \frac{\Psi}{T}dq - \frac{E}{T}dP + \cdots + \frac{\mu_n}{T}dn_n \tag{11}$$

### 2.2.2 Phase Transitions

Biological membranes can go through phase changes between gel and fluid states about 10-15ºC below physiological or growth temperature [6], even though melting temperatures of individual lipid species may vary between -20ºC and 60ºC.

In the gel state, also known as the solid ordered phase, the lipid head groups are tightly packed in a triangular lattice and the hydrophobic tails are in an all-trans configuration. This is the lowest entropy configuration of the lipid bilayer. The fatty acid lengths are maximised and the thickness and surface area of the lipid bilayer are at their minimum.

In the fluid state, also known as the liquid disordered state, the head groups are laterally disordered and the hydrophobic tails can adopt both gauche and trans configurations of the C-C bonds due to higher energies. The entropy is higher and each lipid occupies more surface area as the hydrocarbon tails are not packed closely as in the gel phase. As a result, the lipids and hence the bilayer are shorter due to the shortening of the chain by gauche conformations. It has been shown for DPPC bilayers, that the fluid state experiences a 24.6% increase in surface area and a 16.3% decrease in thickness, in undergoing a gel to fluid phase transition [18].

In theory, other phases such as solid-disordered and liquid-ordered phases can exist and the phase transition described above is a simplification since all head-group and hydrocarbon changes are assumed to occur at the same temperature. However, if we stick to the simple two state model of lipid melting, the melting point $T_m$ is defined as the temperature at which one would find both states with equal probability or alternatively where the Gibbs free energies of the two states are equal:

$$\Delta G = G_{fluid} - G_{gel} = 0 \tag{12}$$

$$H_{0,fluid} - T_m S_{0,fluid} - H_{0,gel} + T_m S_{0,gel} = 0 \tag{13}$$

$$T_m = \frac{H_{0,gel} - H_{0,fluid}}{S_{0,gel} - S_{0,fluid}} \tag{14}$$

The melting temperature depends on the chemical structure of the lipid as well as hydrostatic pressure, the presence of anaesthetics [15], and an external electric field [19], [20] which can (among other effects) change the orientation of the polar head groups.

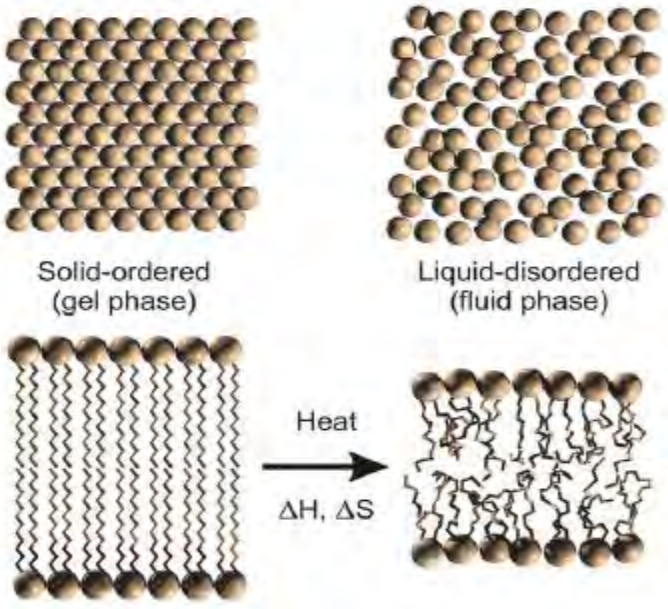


**Figure 4** ***Above:*** Upon a phase transition from solid-ordered phase (left) to liquid-disordered phase (right), the lateral order of the lipid head is broken. ***Below:*** The hydrocarbon chains can fold and occupy more area, in the liquid-disordered phase, thereby reducing the thickness of the membrane [2].

### 2.2.3 Heat Capacity

Heat capacity is the amount of heat absorbed by a material in order to increase its temperature by a given amount. The specific or molar heat capacities are the heat capacity per unit mass and mole of a material, respectively. During phase transitions, the heat capacity peaks because at these points, more heat is required in order to increase the temperature by the same amount as that required farther below or above the melting point. Thus, calorimetry experiments are suitable to determine the melting points of substances. The thermodynamic definition of heat capacity is:

$$c_p = \left(\frac{dQ}{dT}\right)_P = \left(\frac{dH}{dT}\right)_P = T\left(\frac{dS}{dT}\right)_P \tag{15}$$

In equilibrium the lipid bilayer undergoes thermal fluctuations about the melting point. From these fluctuations, very important membrane properties can be derived. For example the heat capacity and enthalpy fluctuations are related:

$$c_p = \frac{d\langle H\rangle}{dT} = \frac{\langle H^2\rangle - \langle H\rangle^2}{RT} \tag{16}$$

It follows that all other susceptibilities are also proportional to the magnitude of fluctuations of their related extensive variable. In the phase transition, the fluctuations are maximised, hence the susceptibilities are maximised. The isothermal volume and area compressibilities are also maximised

## 2.3 Capacitance, Polarisation, Dielectric Constant

Capacitance is a measure of the ability of a system to store electrical charge. A parallel plate capacitor is a system which can store electrical charge. It consists of two parallel conducting planar plates separated by some distance, with an insulating material in between called the dielectric. When the plates are oppositely charged, an electric field forms across them and when the dielectric is placed in this field, it experiences a polarisation in response to the field. This in turn results in a *net* accumulation of charge close to the plates – negative charge close to the positively charged plate and net 'positive' charge close to the negatively charged plate – which reduces the electric field strength of the original empty capacitor. This reduces the potential difference between the plates and the 'charge storing ability' of the capacitor is increased. Therefore, the dielectric material has the effect of increasing capacitance. Mathematically, the capacitance of the capacitor is given by:

$$C = \frac{Q}{V} \tag{17}$$

where $C$ is the capacitance and $V$ is the potential difference. Introducing the material decreases the voltage, which increases the capacitance as the net charge on the plates remains unchanged!

With fixed capacitor geometry, the dielectric constant of the membrane is proportional to the capacitance and gives us a measure of the material's effect on the capacitance. It is the ratio of the absolute permittivity of the dielectric to the permittivity of vacuum ($\epsilon_o \approx 8.854 \cdot 10^{-12}$F/m) which is equal to the ratio of the capacitance of the capacitor with dielectric material to an empty capacitor:

$$\varepsilon_r = \frac{C}{C_0} = \frac{\varepsilon}{\varepsilon_0} \tag{18}$$

where $\varepsilon_r$ is the relative permittivity or the dielectric constant. These terms will be used synonymously in the following..

Permittivity is a measure of how much a material reduces the field across it, namely by becoming polarised. The greater the net polarisation developed by the dielectric material, the greater its dielectric constant. There are different polarisation mechanisms which contribute to the net polarisation which are reviewed in the next section.

For a capacitor with a plate separation distance *d*, the electric field across the dielectric can be expressed as

$$\vec{E} = \frac{\rho}{\varepsilon} \tag{19}$$

where $\rho = \frac{q}{A}$ is the area charge density on the area of plate overlap and $\varepsilon = \varepsilon_0 \cdot \varepsilon_r$. The voltage can be defined as the line integral of the electric field with respect to distance:

$$V = \int_0^d \vec{E} dx = \int_0^d \frac{\rho}{\varepsilon} dx = \frac{\rho d}{\varepsilon} = \frac{qd}{A\varepsilon} \tag{20}$$

So the capacitance of a capacitor with dielectric medium with relative permittivity $\varepsilon_r$ is

$$C = \frac{q}{V} = \frac{q}{\frac{qd}{A\varepsilon}} = \epsilon_o \epsilon_r \frac{A}{d} \tag{21}$$

This means that for a constant relative permittivity, capacitance only depends on the geometry and dimensions of the capacitor.

## 2.4 Electrical Properties of Lipid Membranes

### 2.4.1 Membrane Capacitance

We assume the membrane to be a dielectric material in a parallel plate capacitor with capacitance $C_m$ and voltage $V_m$, where:

$$C_m = \frac{q}{V_m} = \frac{\varepsilon_0 \varepsilon A}{D} \tag{22}$$

where *A* and *D* are the surface area and thickness of the membrane, respectively.

During nerve pulses transient voltage changes occur of the order of 100mV per millisecond. Voltage changes across membranes lead to changes in the charge over time. These are called capacitive currents, given by:

$$\frac{dq}{dt} = \frac{d}{dt}(C_m \cdot V_m) \tag{23}$$

$$\frac{dq}{dt} = C_m \frac{dV_m}{dt} + V_m \frac{dC_m}{dt} \tag{24}$$

In the Hodgkin Huxley electrophysiological model for nerve pulse propagation [8], the membrane capacitance is assumed to be constant, so $\frac{dC_m}{dt} = 0$, and the second term in the equation above becomes zero [21]. Since changes in the geometry of a capacitor change its capacitance, this implies that the geometry of the membrane is fixed during nerve pules. This is however not true since nerve excitations are accompanied by changes in thickness which have been experimentally observed [6] [7] [22] [23]. The thinning of the membrane as it undergoes phase transition, means reducing the thickness of the capacitor which implies an inversely proportional increase in capacitance. Thus the membrane capacitance is a function of any variable that can affect the physical state of the membrane, such as pressure, lateral pressure and voltage.

If we consider a capacitor with all intensive variables, except for voltage, kept constant, we can write the change in charge $dq$ as:

$$dq = \left(\frac{\partial q}{\partial V_m}\right) dV_m = \hat{C}_m dV_m \tag{25}$$

where we have introduced a new quantity $\hat{C}_m = \left(\frac{\partial q}{\partial V_m}\right)$ called the capacitive susceptibility [9], [24].

Using the previous relation $C_m = \frac{q}{V_m}$, we can rewrite this as

$$dq = \left(\frac{\partial (C_m V_m)}{\partial V_m}\right) dV_m = \left(C_m \left(\frac{\partial V_m}{\partial V_m}\right) + V_m \frac{\partial C_m}{\partial V_m}\right) dV_m$$

$$= \left(C_m + V_m \frac{\partial C_m}{\partial V_m}\right) dV_m$$

$$= C_m dV_m + V_m dC_m \tag{26}$$

This equation represents both the changes in the charge on the capacitor due to changes in voltage and also voltage-induced changes in the capacitance, denoted by the capacitive

susceptibility $\hat{C}_m = \left(\frac{\partial q}{\partial V_m}\right) = C_m + V_m \frac{\partial C_m}{\partial V_m}$. At zero voltage, $C_m$ is determined only by the dimensions of the capacitor, which if planar, is given by $C_m = \frac{\varepsilon_0 \varepsilon A}{D}$. However the second term of the capacitive susceptibility is proportional to the voltage and can become significantly large near transitions.

### 2.4.2 Electrostriction

When a capacitor is charged, its conductive plates experience an attractive force, which produces a mechanical force on the capacitor. If the plates are not fixed and the dielectric material is elastic, this can compress the dielectric material in between. This effect is known as electrostriction. In the context of membranes, this is relevant since we are dealing with capacitors with soft matter dielectric material. The work done by electrostriction can affect the phase transitions of membranes, since during phase transitions, the thickness of the membrane changes. The electrostatic nature of this attraction means that this force is quadratically linked to the voltage. A similar effect is reverse piezoelectricity which is an internal mechanical strain generated by en applied electric field, and this is a linear electromechanical interaction.

For a membrane with a uniform dielectric constant in the interior, a fixed thickness *D*, a capacitance $C_m$ and a transmembrane voltage $V_m$, the electric field across it is given by

$$E = \frac{V_m}{D} \tag{27}$$

The charge is given by $q = C_m V_m$. The electrostrictive force on the membrane is given by [25]

$$\mathcal{F} = \frac{1}{2} E \cdot q = \frac{1}{2} \frac{V_m}{D} q = \frac{1}{2} \frac{C_m V_m^2}{D} \tag{28}$$

This force reduces the thickness of the membrane and increases the surface area (assuming a relatively smaller change in volume). These are similar to the changes in dimensions related to lipid melting, so it is reasonable to think that an electrostrictive force can increase the melting temperature of a membrane.

The corresponding work done by the electric field upon melting of the membrane, at constant voltage is

$$\Delta W_C = \int_{D_g}^{D_f} \mathcal{F} dD = \int_{D_g}^{D_f} \frac{1}{2} \frac{C_m V_m^2}{D} dD = \frac{1}{2} V_m^2 \int_{D_g}^{D_f} \frac{\left(\frac{\varepsilon_0 \varepsilon A}{D}\right)}{D} dD$$

$$\Delta W_C = \frac{1}{2} \varepsilon_0 V_m^2 \int_{D_g}^{D_f} \frac{\varepsilon A}{D^2} dD \tag{29}$$

where $D_g$ and $D_f$ are the thicknesses of the membrane for gel and fluid state, respectively.

In the case of the melting of a DPPC bilayer, the surface area increases by 24.6% and the thickness decreases by 16.3%, as mentioned before. It is interesting to note that under the assumption of a constant dielectric constant, the ratio of membrane capacitance for gel and fluid states of the membrane is

$$C_{m,fluid} = \varepsilon_0 \varepsilon \frac{A_g(1+0.246)}{D_g(1-0.163)} = 1.49 C_{m,gel}$$

where $A_g$ is the surface area in the gel phase, and the resulting difference in electrostrictive force is

$$\mathcal{F}_{fluid} = \frac{1}{2}\frac{(C_{m,gel} \cdot 1.49)V_m^2}{D_{gel} \cdot (1-0.163)} = 1.78\mathcal{F}_{gel}$$

Thus the fluid state displays a capacitance about 1.5 times greater and an electrostrictive force 1.78 times greater, than those in the gel state.

The change in enthalpy is

$$\Delta H(V,T) = \Delta H_0(T) + \Delta W_C \tag{30}$$

At $T \gg T_m$, $\Delta H(V,T)$ assumes a constant value of the excess heat of melting. It is a quadratic function of the voltage

$$\Delta H(V,T) = \Delta H_0 + \alpha_0 V_m^2 \tag{31}$$

The melting temperature in the presence of a constant voltage is then

$$T_m = \frac{\Delta H(V,T)}{\Delta S_0} = \frac{\Delta H_0 + \alpha_0 V_m^2}{\Delta S_0}$$

$$T_m = (1+\alpha)T_{m,0} \tag{32}$$

For constant voltages of 100mV, 1V, 10V the melting temperatures have been shown to shift by 11.4mK, 1.14K and 114K, respectively, toward a lower temperature [9], for a DPPC lipid bilayer. The assumption made in these calculations is a temperature independent dielectric constant. The aim of this thesis is to test this assumption.

## 2.5 Oleic Acid

Oleic acid is a monounsaturated fatty acid with a cis-9 isomerism in its hydrocarbon chain. It has the formula $CH_3(CH_2)_7CH{=}CH(CH_2)_7COOH$. It is abundant in nature and a natural constituent of vegetable oils e.g. olive oil, canola, peanut oil.

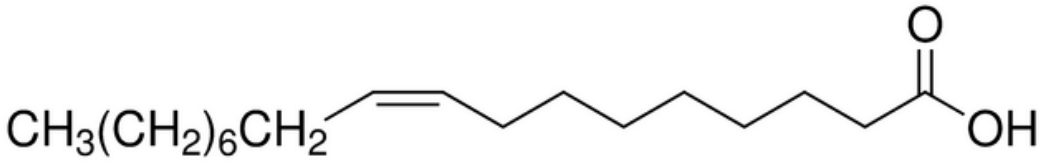


**Figure 5** The Skeletal formula for oleic acid showing the double bond between the 9th and tenth carbons in the chain with a cis-conformation. **[26]**

# 3. Hypothesis

## 3.1 Polarisation

### 3.1.1 Polarisation by an electric field

The dielectric constant of a dielectric is a measure of the lining up of dipoles in a material in the presence of an electric field. Polarisation in a linear, homogeneous and isotropic medium is proportional to the electric field and is given by the following relation

$$\vec{P} = \varepsilon_0 \chi \vec{E} \tag{33}$$

where $\chi$ is the electric susceptibility, $\vec{P}$ is the polarisation density, $\vec{E}$ is the electric field. The polarisation and the electric field are proportional, with the electric susceptibility as a proportionality constant, which depends on the structure of the material, which can be influenced by temperature, and phase change. The electrical susceptibility is related to the dielectric constant by

$$\chi = \varepsilon_r - 1 \tag{34}$$

So with a fixed electric field, any effect on the polarisation by some external variable is proportional to the effect on the dielectric constant of the material:

$$\left|\vec{P}\right| = \alpha \epsilon_r \tag{35}$$

where $\alpha$ is a constant. So from this point on, polarisation and dielectric constant will be used interchangeably, unless otherwise specified.

### 3.1.2 Polarisation Mechanisms

There are three polarisation mechanisms that can occur in dielectric media [27]: electronic polarisation – whereby a dipole is formed between the positively charged nucleus and the centre of the electron cloud of every atom in the material; ionic polarisation – an increase in the present dipole between the anions and cations of an ionic bond (the bond is stretched); and orientational polarisation – polar molecules of the material, which contain permanent dipoles, reorient themselves to be aligned with the electric field. The first of these mechanisms applies to every dielectric material, whereas the second only applies to those with ionic bonds, and the third applies to molecules, covalently or ionically bound, which

contain permanent dipole moments i.e. are polar. Thus, polar or ionic materials will have a much higher polarisability than those without permanent dipoles.

### 3.1.3 Temperature dependence

In addition to the different mechanisms, the ease with which each mechanism acts, could affect the polarisability. For example, when the temperature is increased, the molecules of a material have a higher kinetic energy and the mechanical amplitudes of motion are increased. Therefore an electric field's ability to align the dipoles in the material will decrease. This applies to orientational polarisation.

Whatever the temperature dependence of the polarisability is for a material, it cannot be expected to be continuous due to phase transitions. The polarisation of a material is strongly dependent on its structure and at melting transitions, phase changes occur and the dielectric material's structure changes dramatically, which should result in a corresponding discontinuity in the dielectric constant. There could be other discontinuities than that at the melting temperature, for example the dipoles of a crystalline material 'freezing out' at some temperature well below the melting temperature, suddenly resulting in a much stronger electric field required to realign the dipole moments [28]. For physiological temperatures relevant to biological membranes, only the discontinuity associated with melting temperature will be considered.

Oleic acid is a fatty acid consisting of a polar carboxyl group and hydrocarbon chain with a double bond between the $9^{th}$ and $10^{th}$ carbons with can be in a cis or trans configuration. Because the non-polar chain dominates the overall polarity of the molecule, it is predominantly considered a non-polar molecule, therefore one would expect its temperature dependence to be very small. The literature value for its dielectric constant is about $\varepsilon_r = 2.5$ [29].

The head groups of some phospholipids are charged or zwitterionic, which means that they can have permanent dipoles. Thus, a (artificial) membrane in an ionic aqueous environment can be modelled as a capacitor with two layers of a polar material near the capacitive plates, and a nonpolar layer in between. In this case, the polar head groups would contribute much more to the overall polarisation of the lipid bilayer than the hydrophobic core.

# 4. Materials and Methods

## 4.1 Materials

A list of all the materials and tools used during the course of the experiment:

- Capacitor (described in detail in the next section)

- Differential Scanning Calorimeter (DSC)[1]
- Water bath
- LCR-Meter[2]
- Digital Thermometer
- Thermocouple
- Oleic acid[3] (90% purity)
- Canola oil (standard supermarket sample)
- Magnetic Stirrer
- Vacuum pump
- Purified, deionised water
- Ethanol
- Beakers, syringes, freezer and other lab paraphernalia

Graphing softwares: Igor Pro Version 6.3, Excel.

## 4.2 Methods

### 4.2.1 Differential Scanning Calorimetry

A Differential Scanning Calorimeter was used to determine the melting temperature range of oleic acid, in order to know which capacitance measurements could be associated to phase transition.

The Differential Scanning Calorimeter (DSC) contains two cells, in one of which a sample is inserted – in this case oleic acid – and in the other a reference – in this case water was used. The cells are enclosed by a box which controls that no heat is exchanged between that cells and the environment. The temperatures of both cells are changed at a fixed rate by two Peltier heaters such that the temperature of both cells is the same throughout. The DSC then records the difference in the power used to heat or cool these cells as a function of temperature and gives a 'calorimetric profile' from which melting processes can be deduced by peaks in the curves showing power differences between the cells.

[1] type VP-DSC produced by Microcal (Northhampton/MA, USA)
[2] ATLAS LCK model LCR40
[3] Supplier: Sigma-Aldrich Co. LLC. Technical grade: 90%. Among the impurities are: palmitic acid-PA and linolenic acid-LA.

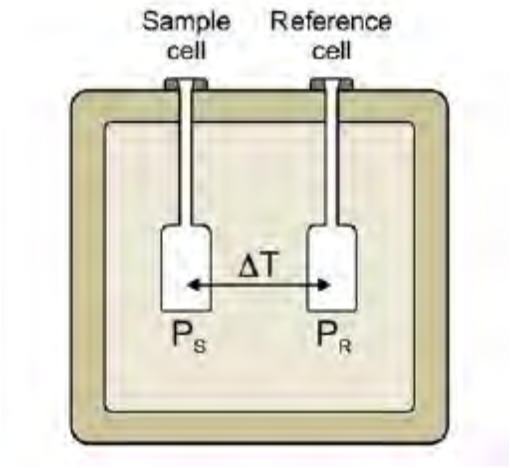


**Figure 6** A diagram of the inside of the calorimeter showing the reference and sample cells. **[30]**

### 4.2.2 Capacitor

The purpose of this investigation was to determine the temperature dependence of the dielectric constant of a material similar to that typically found in the hydrophobic core of lipid bilayers of cell membranes. To this end, a capacitor with plates of known geometry and dimensions (shown below), designed by Karis Zecchi [30], Dennis Wistisen and Thomas Heimburg (Membrane Biophysics Group, Niels Bohr Institute), was filled with oleic acid and the capacitance was measured with an LCR-meter at different temperatures regulated by a water-bath, from which the dielectric constant was evaluated using the relation $C = \epsilon_o \epsilon_r \frac{A}{d}$. This capacitor is shown and described below.

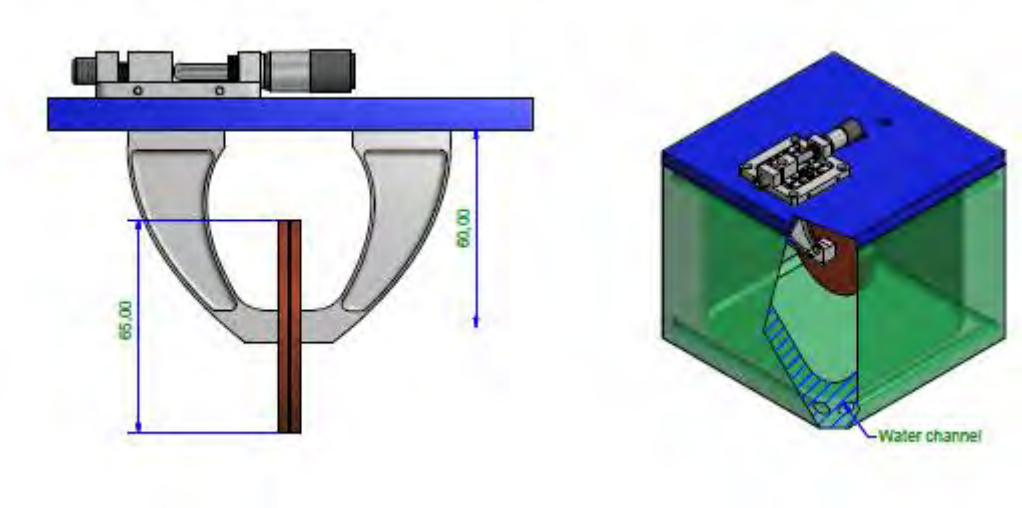


**Figure 7 Capacitor Diagram.** ***Left*****:** a side view of the top lid of the capacitor. One can see the micrometer screw at the top which is attached to a spring which adjusts the plate separation distance to a precision of 10µm, across a range of 2 mm. It does this by moving one of the mounting brackets underneath the lid, to which the conducting discs are attached. The two capacitor disks of 65mm diameter are made of copper and are horizontally aligned with their planes parallel. To each plate, an electrode is attached to allow for capacitance measurements. ***Right:*** The entire assembled structure of the capacitor is shown with the lid screwed onto the box. The capacitor plates are thus suspended in a cavity (with a capacity of about 1.7 litres) which can be filled up with a liquid, thus completely

engulfing the plates. The box itself is also hollow and has two insulated tubes (not shown) linked to channels within the hollow interior, one of which protrudes at the top of the box and the other at the bottom, to allow for a water-bath regulated temperature control of the liquid in the cavity. The box (including the lid) is made of aluminium, thermally and electrically insulated by a black anodised surface treatment. The technical drawing and the realisation of the capacitor were made by Dennis W. Wistisen.

### 4.2.3 Plan

With this setup, the principle of the method is the following.

1) Differential Scanning Calorimetry

   Using the DSC, determine the melting range of oleic acid. For the reference cell, use water.

2) Calibrating the Capacitor

   a) Effective 'zero' on micrometre screw:

   Connect the electrodes of the LCR-meter to those of the capacitor. Starting with the capacitor plates merged, gradually increase the plate separation distance while measuring the capacitance in order to find the effective zero distance on the micrometre scale. This is the point where capacitance first takes a finite value.

   b) Determining effective capacitor area of plate overlap $A_{eff}$:

   Measure and record the capacitance (dependent variable) at 50 µm intervals, for a range of plate separation distance (independent variable) from 50-2000 µm (from the effective zero distance). Plot capacitance over distance and fit to the following function

$$C(d) - C_0 = \frac{\kappa}{d - d_0} \tag{36}$$

   where $\kappa = \varepsilon_0 \varepsilon_r A_{eff}$, $C(d)$ represents the capacitance and $d$ represents the plate separation distance. The fit curve is an inverse function with symmetry about $C(d) = d$. Using the fit, $C_0, d_0$ and $A_{eff}$ can be determined as $\varepsilon_0$ is known and $\varepsilon_r \cong 1$ for air. The same process can be repeated by assuming that the area is much bigger than the plate separation and edge effects are negligible (the capacitor was designed with this objective [30] ), and using the known dimensions of the capacitor plates one can determine $\varepsilon_0$ to compare to the literature value of $\varepsilon_0 \approx 8.854 \cdot 10^{12}$F/m.

3) Measurement

   Fill the capacitor with fluid of interest. The fluid must be degassed with a vacuum pump to remove dissolved air. Control the temperature with a water bath. For each fixed temperature, measure the capacitance as described in 1 a) and b) to determine $\varepsilon_r$.

   This was first tested with water and canola oil and afterwards measurements were made for oleic acid.

4) Control

   To control for changes in the dimensions of the copper plates with temperature, repeat 1) for different temperatures to determine changes in $A_{eff}$.

In between all the steps, the capacitor must be cleaned with water and ethanol, and dried.

## 4.3 Obstacles and changes in the setup

As this experimental setup is new and has never been used before, numerous obstacles were discovered throughout, some of which are mentioned here.

**Calibration**

Error relating to the direction of twist on the micrometre screw was controlled for by checking that the capacitance recorded was the same regardless of the direction of twist used to fix the plate distance. Error relating to the LCR-meter, was controlled by repeating measurements for each fixed distance, giving an error of 1-3 pF.

**Canola oil**

**Problems:**

Temperature gradients within the sample were observed. Bringing the thermometer close to the plates gave a different temperature reading to that recorded when letting it rest in the corner of the cavity. Furthermore, the lid was open the whole time as there was no other way to record temperature.

The copper electrodes had developed turquoise areas on the surface. This was assumed to be corrosion due to contact with water.

**Solutions/modifications:**

Manual stirring was employed to reduce temperature gradients in the sample, but in order to stir one had to open and close the lid all the time, which made temperature fluctuations even greater as the sample was more exposed to room temperature.

To avoid copper corrosion, the capacitor was henceforth cleaned only with ethanol.

**Oleic Acid**

**Problems:**

During phase transition, the temperature first reached a minimum of about 11.4 ºC and then increased to about 14ºC, after which it descended again at a much slower rate. Throughout, the water bath temperature was kept constant at 10.8 ºC. Due to these fluctuations, it was impossible to keep a steady temperature for measurements, and it was difficult to pinpoint the exact melting temperature of the oleic acid[4].

[4] A precise melting temperature or melting 'point' is an ideal notion. There is always phase coexistence at a specified temperature range, which depends on the rate of temperature change. In especially large samples as this (about 1.7litres) the phase coexistence range is expected to be large. Furthermore, literature values for the melting point of oleic acid vary from 11.5-13.5

After phase change, temperature reduction occurred at a much slower pace. Lowering the water bath temperature down to –3 ºC resulted in an average 0.1 ºC temperature change per hour.

When the sample solidified at 12ºC changing the capacitor plate distance was impossible.

**Solutions/modifications:**

A magnetic stirrer was used to replace manual stirring.

The thermometer was replaced by thermocouple, which could be immersed in the sample and fixed near the centre of the capacitor plates, *without* removing the lid. It was connected to an amplifier and temperatures were monitored henceforth at 10 second intervals during experiments.

The measurement procedure was modified, to allow for solidification. Instead of fixing temperatures and taking capacitance measurements at different inter-plate distances, the distance was fixed and capacitance was measured for different temperatures.

Heating something is generally easier than cooling it[5] so henceforth, samples were first cooled using the water bath and then measurements were taken as the system was gradually heated.

**Problems:**

Removal of the capacitor lid revealed an unrelenting formation of bubbles in the sample, which both appeared to nucleate from the walls of the capacitor cavity and the copper plates.

Reducing the temperature of the oleic acid to below ~10 ºC using a water bath proved ineffective. The decrease in temperature after solidification, reached a terminal speed of 0.1 º/hour.

Temperature fluctuations were greater using the magnetic stirrer.

**Solutions:**

The magnetic stirrer was removed from the setup, with the speculation that the additional convection of heat it produces in the sample, may contribute to the formation of bubbles *and* to reduce temperature fluctuations at phase transition.

The sample was frozen in a freezer at fixed plate distances (instead of using the water bath) in order to reach temperatures below 10 ºC and get capacitance recordings for the solid state, well below the melting point.

[5] Increasing the temperature of a system means increasing its entropy. If entropy is thought of as a measure of disorder then creating disorder is 'easier' than creating order. This is not entirely correct however, a comfortable analogy for current experimental purposes.

Initially, the sample was frozen and thawed several times to see if this would reduce air bubbles. However, bubbles continued to form obstinately, and a small layer of foam appeared on the surface of the sample.

# 5. Results

## 5.1 Calorimetric profile

DSC calorimetry performed at a rate of 0.5º/hour for a temperature range 5-13ºC, revealed a melting temperature range 10.6ºC< $T_m$ <11.6ºC. Below is the calorimetric profile obtained:

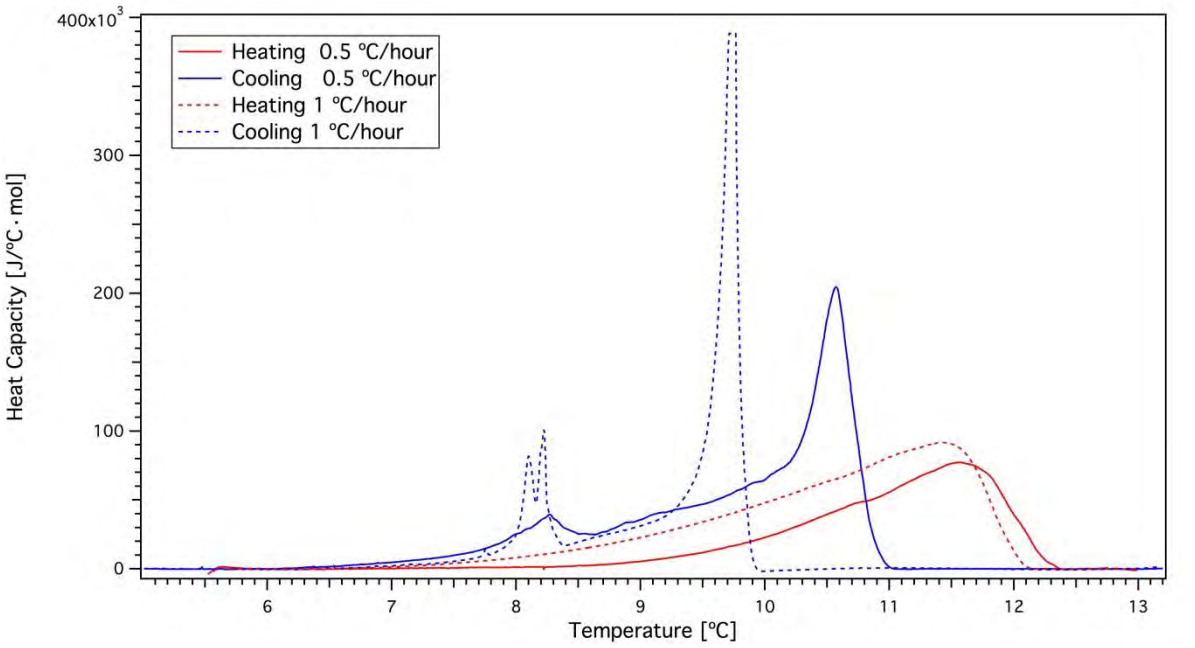


**Figure 8** Calorimetric profiles for oleic acid (90% pure) performed at a rate of 0.5º/hour (solid curves) and 1º/hour (dashed curves). The horizontal axis shows temperature / ºC. The vertical axis shows heat capacity. The approximate phase transition range derived from this is the difference between the peaks of heating (red) and cooling (blue) at 0.5º/hr.

The system shows significant hysteresis, as well as a shift toward higher temperatures as the scan rate is reduced. The additional smaller peaks just above 8°C in the calorimetric profile in Figure 8, may be attributed to the impurities in the oleic acid. DSC calorimetry has also been performed on oleic acid by Sousa *et al.* [31] 60%, 90% and 99% purity. Their results also show additional peaks due to impurities.

## 5.2 Calibration in air

**Effective area:**

Fit function:

$$C(d) = \frac{\kappa}{d - d_0} + C_0, \qquad \kappa = \varepsilon_o \varepsilon_r A_{eff} \tag{37}$$

where $\varepsilon_o = 8.854 \cdot 10^{-12}\text{Fm}^{-1}$ and $\varepsilon_{air} \approx 1$.

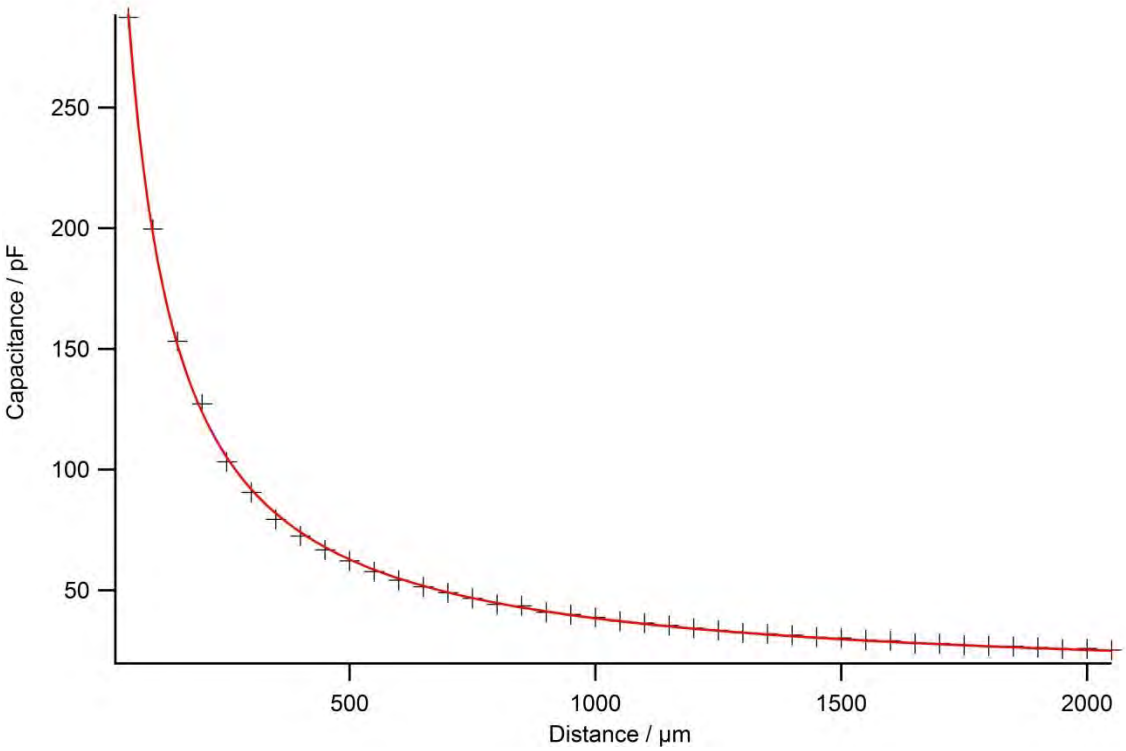


**Figure 9** Graph showing the plotted data for the empty capacitor and corresponding fit function.

Results ('±' refers to standard deviations):
$\kappa = 28311 \pm 275\ \text{pF} \cdot \mu\text{m}$
$d_0 = -52.145 \pm 1.09\ \mu\text{m}$
$C_0 = 11.498 \pm 0.321\ \text{pF}$

$\boldsymbol{A_{eff} = 3.198 \cdot 10^{-3}\text{m}^2 = 31.98\text{cm}^2}$

**Permittivity of free space ($\varepsilon_o$):**

Using the same fit, and the known dimensions of the capacitor disc:

area disc = $A_{theoretical} = \pi r^2 = \pi \cdot (3.25\text{cm})^2 = 33.18\text{cm}^2$

we derive a value for $\varepsilon_0$:

$$\kappa = \varepsilon_0 \varepsilon_{air} A_{theoretical} = \varepsilon_0 \cdot 1 \cdot \pi \cdot (3.25\text{cm})^2$$

$$\varepsilon_0 = \frac{\kappa}{\pi \cdot (3.25\text{cm})^2} = \frac{28{,}311\ \text{pF} \cdot \mu\text{m}}{\pi \cdot (3.25\text{cm})^2}$$

$$\boldsymbol{\varepsilon_0 = 8.532 \cdot 10^{-12}\ \mathrm{Fm^{-1}}}$$

$$\text{Relative error} = \left(1 - \frac{8.532 \cdot 10^{-12}\mathrm{Fm^{-1}}}{8.854 \cdot 10^{-12}\mathrm{Fm^{-1}}}\right) \cdot 100 = 3.64\%$$

### 5.3 Water

The LCR-meter displayed capacitance values of many orders higher than those expected for water and the values were not constant. This can be attributed to the fact that water is very difficult to deionise completely and the sample still contained ions after it was deionised, which implies that there was conductance between the capacitor plates. Since there is no economical solution to this problem, this step was abandoned.

### 5.4 Canola oil; liquid phase

Now we use the value for the effective area of the capacitor found in the previous section in the fit equation, and derive the relative permittivity of canola at 10ºC, 20ºC and 30ºC:

$$C(d) = \frac{\kappa}{d - d_0} + C_0, \qquad \kappa = \varepsilon_o \varepsilon_r A_{eff}, \qquad A_{eff} = 3.198 \cdot 10^{-3}\mathrm{m^2}$$

$$\varepsilon_r = \frac{\kappa}{\varepsilon_o A_{eff}} \tag{38}$$

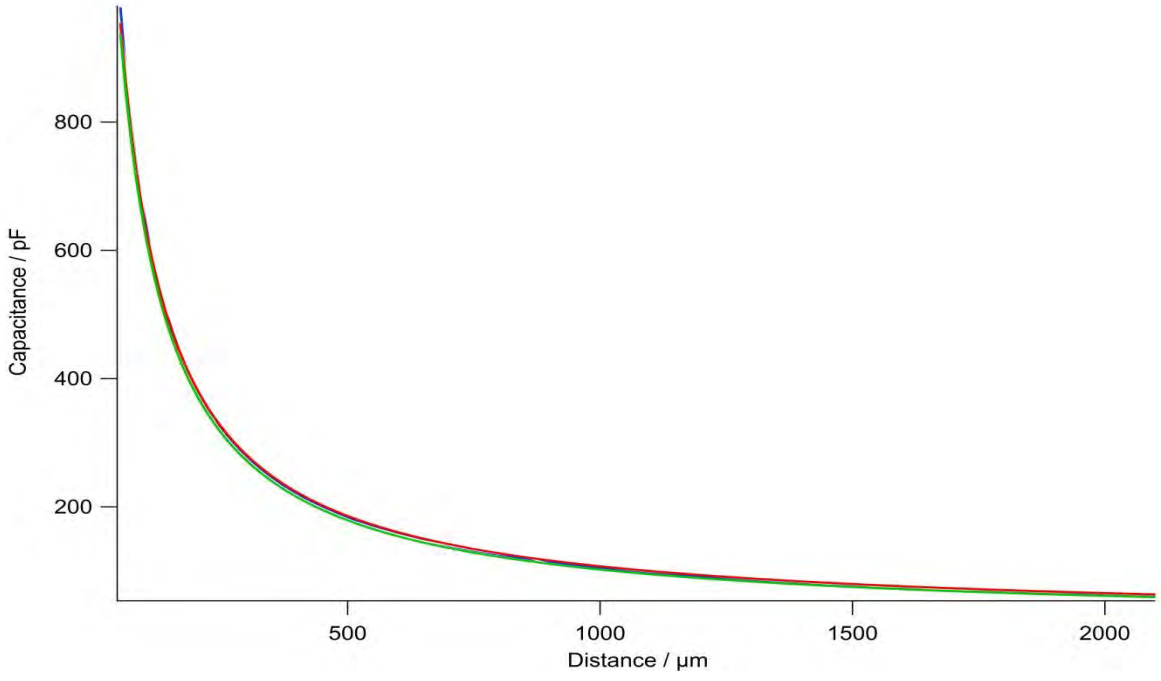


**Figure 10** Graph of the three fit functions for canola at 10ºC (red curve), 20ºC (blue curve), and 30ºC (green curve). Without explicitly deriving the dielectric constants for the three temperatures, one can already see that the differences will be very small as the curves are so tightly packed together – the blue curve is hidden by the red and green curves, and only its upper tip is easily noticeable. One can also see that the capacitances for 10ºC canola (red curve) are higher than those of 30ºC canola (green curve) and those of 20ºC canola (blue curve) are in between , implying that the dielectric constant decreases slightly as temperature is increased.

The values (with propagated error) obtained for the dielectric constants of canola at different temperatures are:

$$\boldsymbol{\varepsilon_r(10°C) = 3.17 \pm 0.12}$$

$$\boldsymbol{\varepsilon_r(20°C) = 3.12 \pm 0.11}$$

$$\boldsymbol{\varepsilon_r(30°C) = 3.09 \pm 0.11}$$

One can speculate that the dielectric constant decreases as temperature is increased, however three data points are not enough to discuss the nature of this relation (i.e. linear, logarithmic…) any further, and the smallest propagated error is greater than the difference between any two values.

### 5.5 Oleic Acid; liquid phase

The relative permittivity values ($\varepsilon_r$) are determined for oleic acid in liquid phase at temperatures 13ºC, 14ºC, 16ºC, 20ºC, 30ºC, 40ºC. Due to large error for capacitor plate separation distances of 50µm and 100µm, their corresponding capacitance values are omitted. The large error is probably due to the great effect of capacitor plate misalignment at small separation distances. Results are for the separation distance range $150\mu m \leq d \leq 2000\mu m$. This is also reasonable for the fit function – an inverse function with reflective symmetry about a diagonal line.

For $150\mu m \leq d < 1000\mu m$ measurements were taken at 50µm intervals and for $1000\mu m \leq d \leq 2000\mu m$ the intervals were 100µm. Measurements for 12 ºC were also omitted as this is when a phase transition took place and temperature fluctuations occurred.

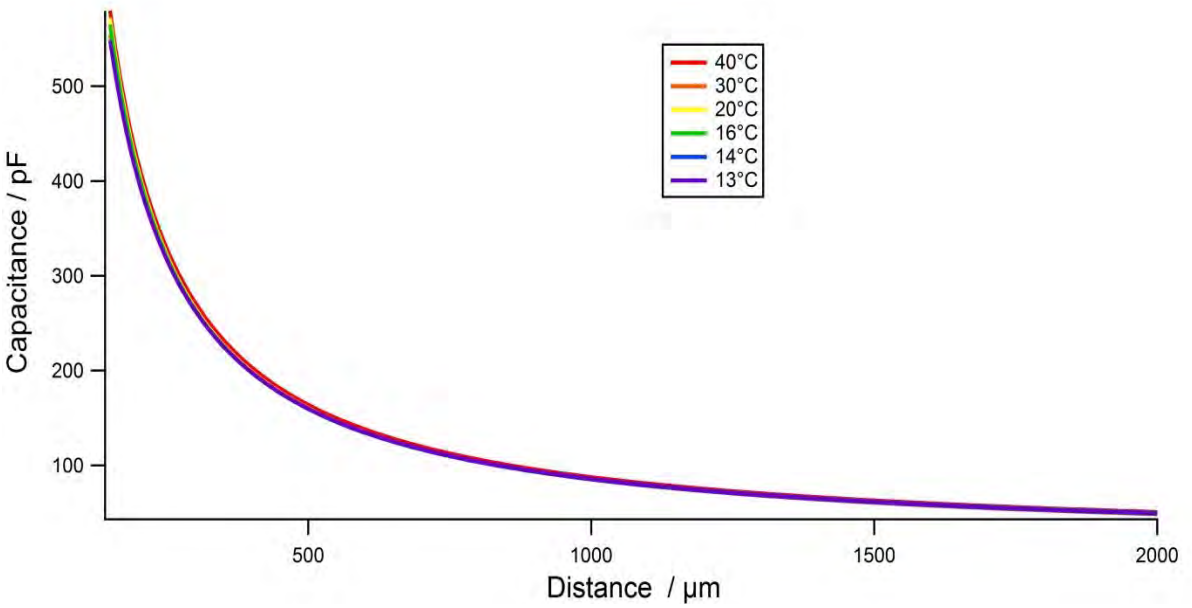


**Figure 11** The fit function for the plotted values (not shown) for oleic acid in liquid phase at temperatures 13ºC, 14ºC, 16ºC, 20ºC, 30ºC, 40ºC. A legend is presented to show which temperatures correspond to which curves. The curves are very tightly packed, implying little difference in dielectric constant as temperature is changed.

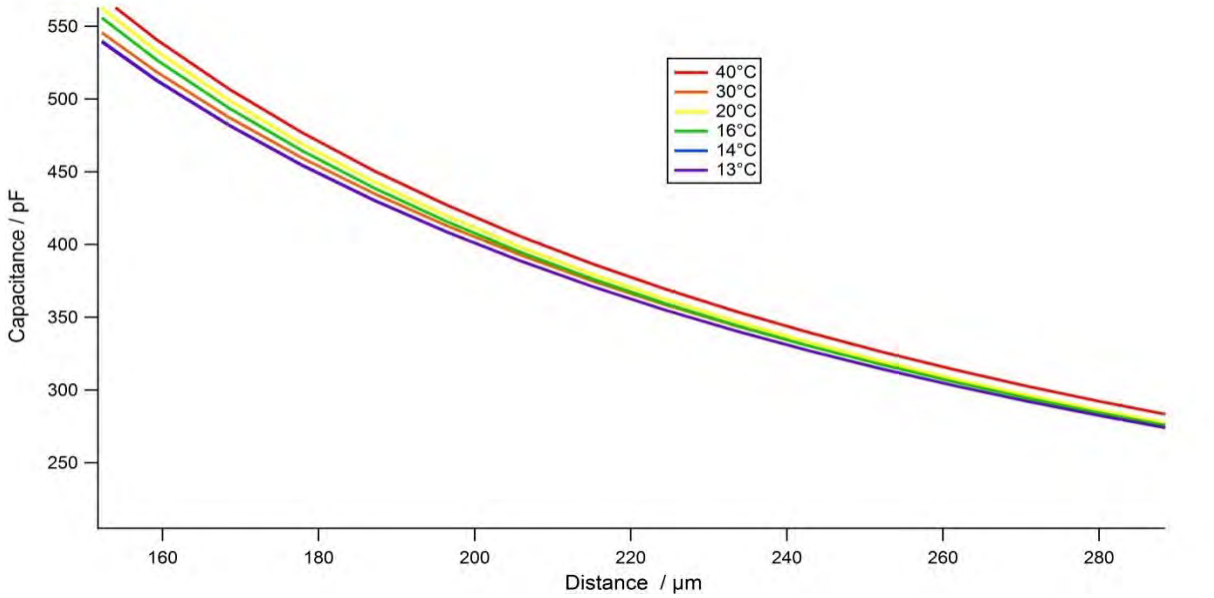


**Figure 12** A zoom-in on the graph in Figure 11 The fit function for the plotted values (not shown) for oleic acid in liquid phase at temperatures 13ºC, 14ºC, 16ºC, 20ºC, 30ºC, 40ºC. A legend is presented to show which temperatures correspond to which curves. The curves are very tightly packed, implying little difference in dielectric constant as temperature is changed..

From the fitted curves, values for $\kappa$ are obtained and corresponding values for the dielectric constant are calculated using the relation $\varepsilon_r = \frac{\kappa}{\varepsilon_0 A_{eff}}$, where $\varepsilon_0$ and $A_{eff}$ are known:

| **Dielectric constant $\varepsilon_r$** | **Temperature / ºC** | **Temperature / K** |
|---|---|---|
| 2.48 | 13 | 286 |
| 2.48 | 14 | 287 |
| 2.42 | 16 | 289 |
| 2.42 | 20 | 293 |
| 2.52 | 30 | 303 |
| 2.50 | 40 | 313 |

**Table 1** The derived values of dielectric constant at different temperatures for liquid oleic acid

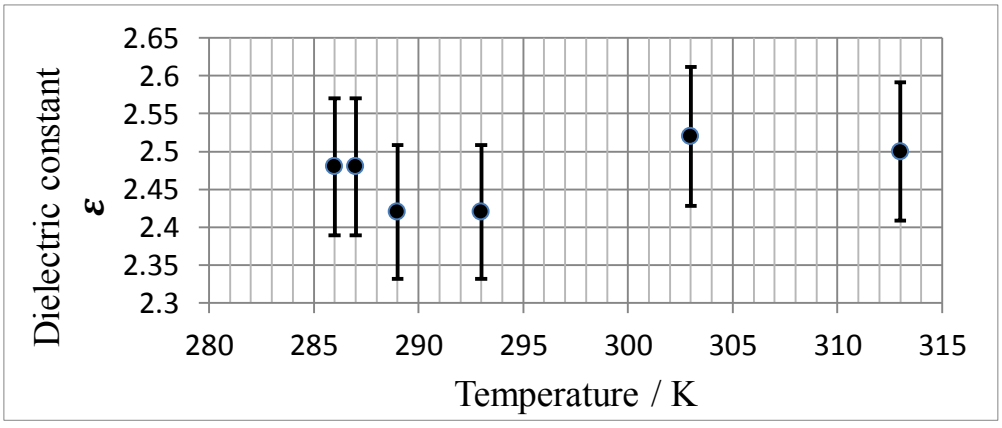


**Figure 13** Plot of data in Table 1, with error bars representing the propagated error.

All the error bars overlap, which means that no differences in the values for dielectric constant can be concluded. The greatest difference between values is 0.10 (between $\varepsilon_r(20°C)$ and $\varepsilon_r(30°C)$ which corresponds to ~4% increase.

The conclusion is that there is no discernible change in dielectric constant with temperature which can be measured within the precision of the method, in the liquid phase.

### 5.6 Oleic acid; liquid and solid phases

Using the relation $\varepsilon_r = \frac{(C-C_0)\cdot(d-d_0)}{\varepsilon_0 A_{eff}}$, where $C_0, d_0$ are the fit constants obtained for the capacitor in air at $T \approx 20°C$, the dielectric constants at the fixed distances are calculated:

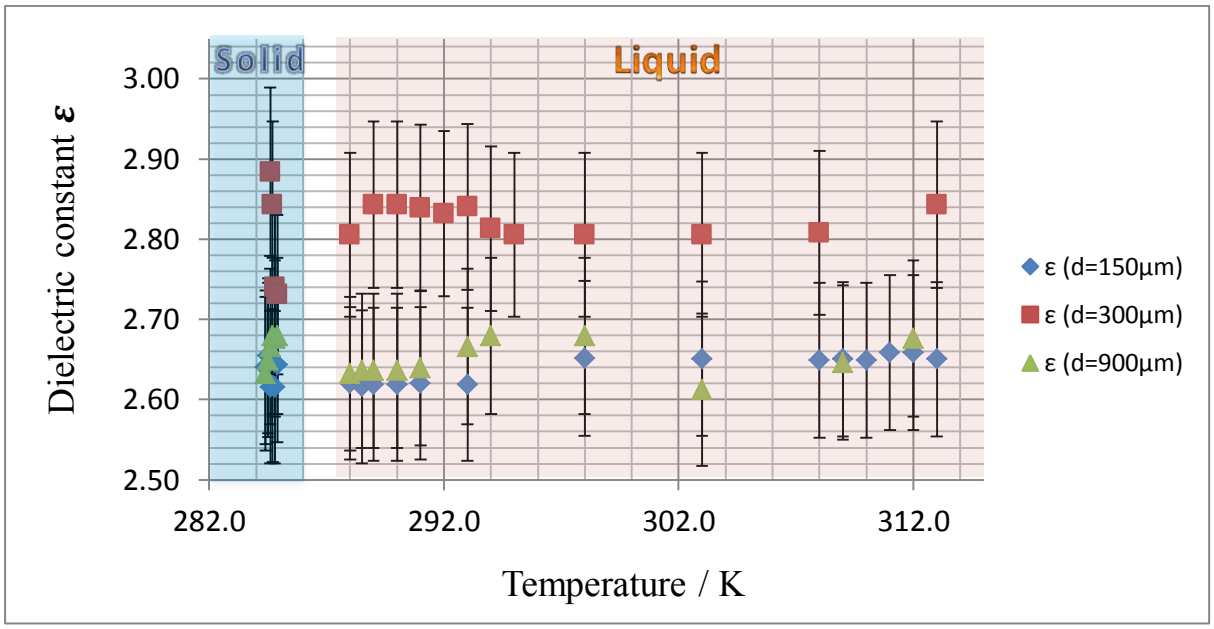


**Figure 14** Plotted values of dielectric constant with temperature (in Kelvin) for plate separation distances 150µm, 300µm and 900µm The values are for oleic acid in 100% solid (blue shade) and 100% liquid (red shade) phases only.

From Figure 14, one can see that the variation in dielectric constant with temperature is very small. There is no change with temperature as all the plotted values are within range of every other error bar. Nevertheless a difference in dielectric constant with plate separation distance can be observed, particularly for 300µm

The small difference in dielectric constant with plate separation distance could be attributed to the assumption that the effective capacitor disc area determined during calibration is the same for all dielectric materials, for all distances and for all temperatures. This is the same as assuming no changes in 'edge effects' (anisotropy of electric filed flux between the plates, near the edges) as the plate separation distance is increased. However, if this were the case, then one would expect a much bigger change in dielectric constant from 150µm to 900µm than from 300 µm to 900 µm, whereas here the exact opposite is observed.

### 5.7 Oleic acid; liquid phase, phase transition & solid phase

The same method as that used in the previous section is used to determine the dielectric constant dependence of oleic acid at a fixed 900µm plate distance for temperatures at which oleic acid is solid, undergoes phase transition and liquid. Results:

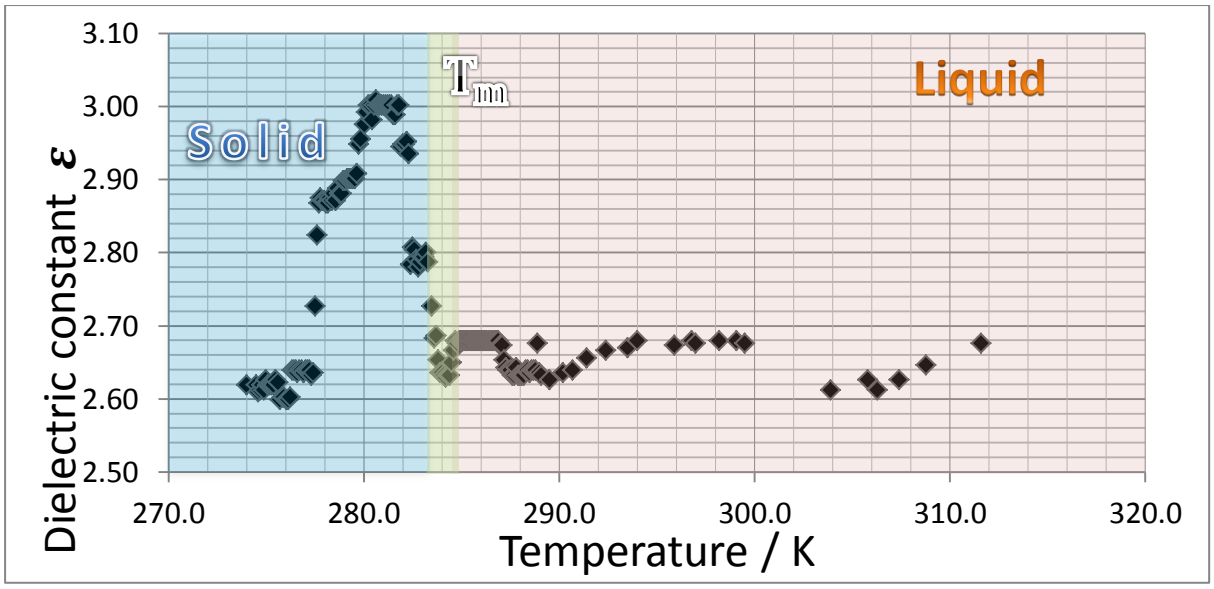


**Figure 15** Plotted values of dielectric constant with temperature. $\mathbf{T_m}$ denotes melting temperature range (green strip in between solid and liquid).

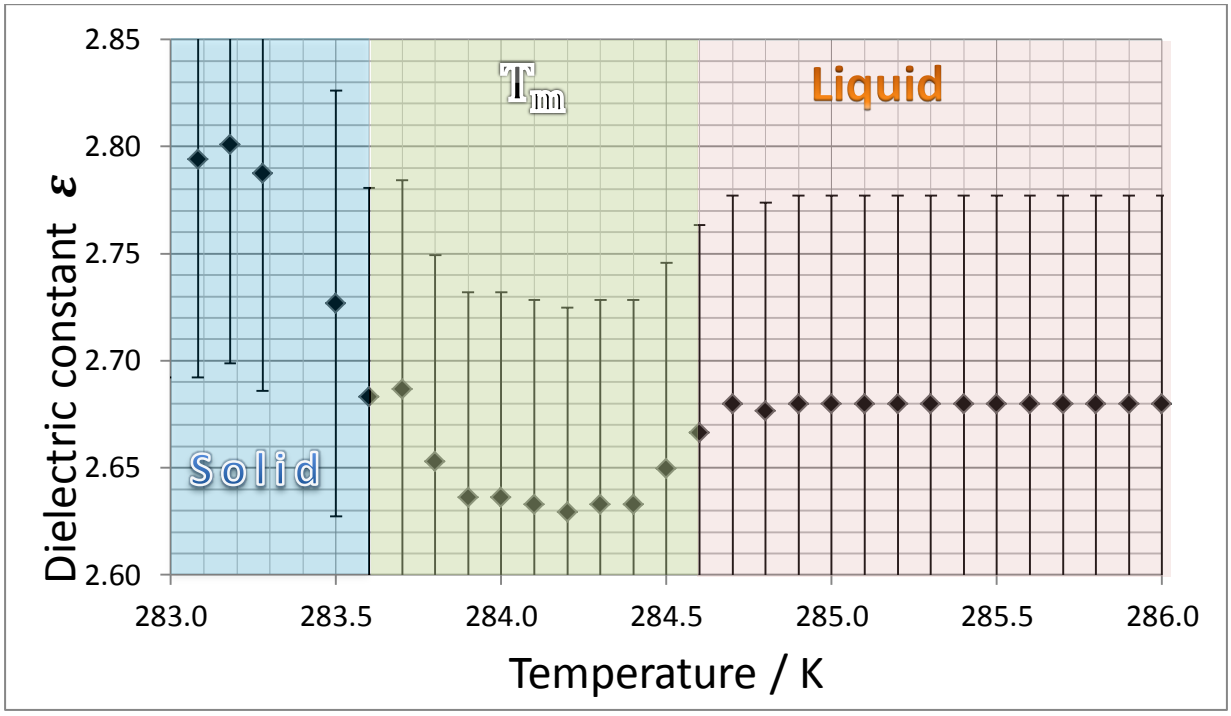


**Figure 16** A zoom-in on the phase transition temperature range of Figure 15, showing the three phases of the oleic acid. $\mathbf{T_m}$ denotes the melting temperature range given by the difference in peaks of the 0.5°/hr cooling and heating curves of the DSC calorimetric profile for oleic acid.

Figure 15 displays a sharp rise in the dielectric constant from about 2.64 to a peak at about 3.00 in the solid phase, followed by a sharp fall. During the phase transition, there is a local minimum at $\varepsilon \approx 2.63$ (Figure 16), followed by a steady value of 2.68 in the liquid phase. At higher temperatures in the liquid phase, the values fluctuate between 2.60 and 2.68.

It is unclear why there is a peak in the solid phase at 280-282 K (7-9°C) (Figure 15). One possibility is that it is associated to the melting range of the impurities in the oleic acid, as it is only 90% pure. The peak's temperature range corresponds to the anomalous extra peaks observed in the calorimetry profile (Figure 8), which were also associated to impurities.

The minimum observed in the melting transition (Figure 16) happens across exactly the same temperature range as the difference in peaks of the 0.5º/hr cooling and heating curves of the DSC calorimetric profile for oleic acid. This implies an inverse proportionality between dielectric constant and heat capacity during transition. However, since all differences between dielectric values in this range are within range of propagated error ($\delta\varepsilon_r \approx 0.11$) one cannot make this conclusion. Thus there is no discernible change in dielectric constant with temperature.

One would have to repeat the experiment for at least 10 fixed distances in order to the use the fit function for different temperatures and conclude something more specific.

# 6. Discussion

## 6.1 Theoretical Calibration for copper expansion

Among the tasks originally planned, one which was not executed but which could have a significant effect on all the results, is taking into account the thermal expansion of capacitor plates. This can affect the effective distance between capacitor plates. A theoretical calculation can give an idea of how much this calibration could affect results. Details of the calculation can be found in the appendix. The results are given below for the values plotted in Figure 14 for oleic acid.

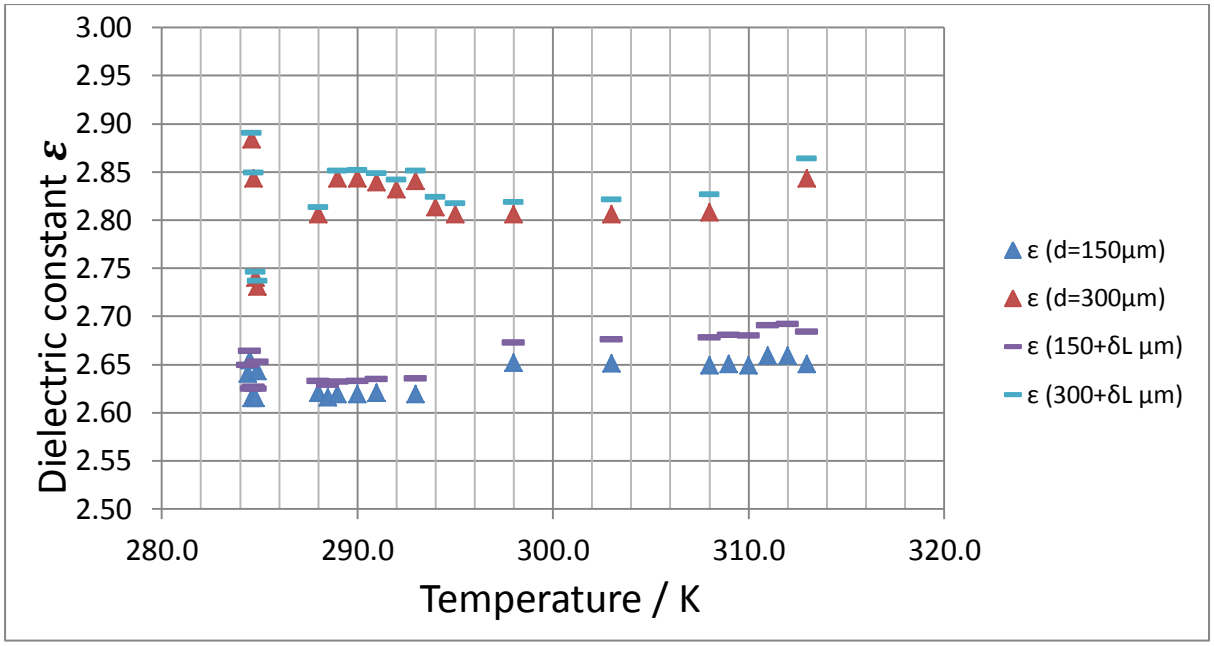


**Figure 17** Plotted values of dielectric constant with temperature (in Kelvin) for plate separation distances 150μm and 300μm (from Figure 14) (triangles) and corresponding thermal expansion calibrated values (dashes)

One can see that the resulting difference is small for small distances (150μm and 300μm). The difference is almost unnoticeable for larger distances.

### 6.2 Modifications to the experimental setup to improve results

- Shortening and insulation of tubes connecting the capacitor to the water-bath. This would greatly reduce the amount of time used trying to equilibrate water bath and capacitor temperatures, and would make the temperature much more controllable
- An automated procedure which can be pre-set to record capacitance and control temperature. One could economise an immense amount of time and achieve much more accurate results. With such a system, the capacitor would be more accessible and practical for many areas of research (as the DSC), in which one considers temperature dependent dielectric constants of a material of interest.
- In addition to the vacuum pump, one could use a sonicator to remove as much dissolved gas as possible from the sample, prior to experimenting.

## 7. Conclusion and outlook

The results show no consistent, significant change in the dielectric constant with temperature for oleic acid. This is a result in itself, as one can confirm that the assumption of temperature independent dielectric constant in processes involving the biological membrane is reasonable. The complete picture is of course much more complicated. Biological membranes are neither longitudinally nor transversely homogeneous and isotropic, and even

if we just consider single lipid specie vesicles, we would have to consider the dielectric contributions of both the hydrophobic tails and the head groups, which, if polar (for example, in the instance of phospholipids with zwitterionic head groups), can be expected to have a much more dominant dielectric contribution as the net polarisability is higher in material with permanent dipoles. Furthermore, at physiological temperatures one would also have to consider polar head group reorientation as a result of phase transition and/or reorientation induced by transmembrane potential [32], both of which change the structure of the lipids and hence the polarisability. These are just some of the factors involved in the complete picture for membranes and taking everything into account would result in very complicated models. In this project a simple model for membrane dielectric properties has been investigated experimentally.

The temperature dependence of the dielectric constant of oleic acid has been measured before by F. F. de Sousa *et al.* (who also used capacitance measurements with a different experimental setup. For details, see [33] and [34]), where for the same 90% pure sample of oleic acid the following results were obtained

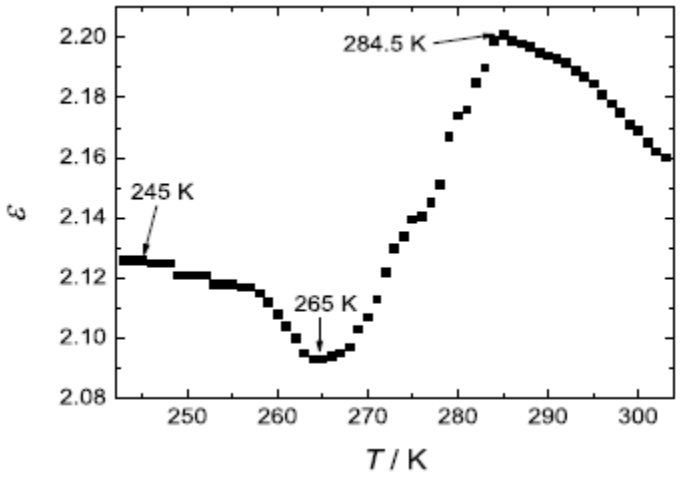


**Figure 18** Dielectric constant plotted against temperature (K) for 90% oleic acid.

The changes in dielectric constant observed here are smaller than the precision of our setup.

In the context of electrostriction in membranes, in [9] (Thomas Heimburg, 2010) the dielectric constant was assumed to be constant and in [30] (Karis Amata Zecchi, 2013) the assumption of proportionality between enthalpy change and change in dielectric constant for a DPPC lipid membrane, with the dielectric constants $\varepsilon_f = 4$ and $\varepsilon_g = 2$ in fluid and gel states, respectively, yielded a shift of less than 8 mK (towards a lower temperature) for the melting temperature, for a physiological transmembrane voltage of $V_m = 100\text{mV}$. The net change in dielectric constant between the two states used here is much greater than any net dielectric changes with temperature observed in this experiment and those observed by *Sousa et al.*(2010) [33] for 99% oleic acid, who found a total decrease in dielectric constant from $\varepsilon_r = 2.50$ to $\varepsilon_r = 2.03$, from $T = 289\text{ K}$ to $T = 298\text{ K}$ in liquid state. Thus, for all future considerations there is evidence to support the assumption of a temperature independent dielectric constant.

On a final note, the capacitor used in the experiments of this investigation is very well designed for its purpose and with the suggestions mentioned earlier, to optimise it, temperature dependence of dielectric constants can be determined for a variety of fatty acids and other materials, over time. The resulting data will have applications in many scientific fields, especially in material science, where currently, research in renewable sources of energy is a high priority. In this context, the investigation of dielectric properties of oleic acid is a good start as it is one of the most abundant naturally occurring fatty acids in nature.

# Acknowledgements

I am extremely grateful to my supervisor, Thomas Heimburg, for giving me this project and for the opportunity to work in the Membrane Biophysics Group. His original take on science has greatly inspired me to not forget that science is not only maths and citations, but also something that, at its best, requires a certain measure of naïve curiosity.

I am exceedingly grateful to my supervisor, Karis Amata Zecchi, who, at all times, helped and supported me generously and for being one of the very few people I know, who are able to answer questions pertaining to the most *fundamental* principles in physics.

Big Thanks to the rest of the group for their unconditional support in the lab and for their very helpful suggestions.

Finally, I am grateful for my friends and family, without whom, nothing exists.

# References


[1] P. W. Kuchel and G. B. Ralston, Theory and problems of biochemistry, New York: Schaum's Outline/McGraw-Hill, 1988.

[2] A. Blicher, "PhD Thesis Electrical aspects of lipid membranes," Niels Bohr Institute, Copenhagen University, Copenhagen, 2011.

[3] S. Paula, A. Volkov and D. Deamer, "Permeation of halide anions through phospholipid bilayers occurs by the solubility-diffusion mechanism," *Biophys J,* vol. 74, no. 1, pp. 319-327, 1998.

[4] I. P. Sugar and E. Neumann, "Stochastic model for electric field-induced membrane pores electroporation.," *Biophysical Chemistry,* vol. 19, no. 3, pp. 211-225, 1984.

[5] T. Heimburg, "Lipid ion channels," *Biophys. Chem.,* vol. 150, pp. 2-22, 2010.

[6] T. Heimburg and A. D. Jackson, "On soliton propagation in biomembranes and nerves," *Proc. Natl. Acad. Sci. USA,* vol. 102, pp. 9790-9795, 2005.

[7] K. Iwasa and I. Tasaki, "Mechanical changes in giant squid axons associated with production of action potentials," *Biochem. Biophys. Res. Commun. ,* vol. 95, pp. 1328-1331, 1980.

[8] A. L. Hodgkin and A. F. Huxley, "A quantitative description of membrane current and its application to cunduction and excitation in nerve," *J. Physiol,* vol. 116, pp. 449-472, 1952.

[9] T. Heimburg, "The Capacitance and Electromechanical Coupling of Lipid Membranes Close to Transitions: The Effect of Electrostriction," *Biophysical Journal,* vol. 103, p. 918–929, 2012.

[10] A. Petrov, "Electricity and mechanics of biomembrane systems: flexoelectricity in living membranes," *Anal. Chim. Acta,* vol. 568, pp. 70-83, 2006.

[11] E. Gorter and F. Grendel, "On biomolecular layers of lipoids on the chromocytes of the blood," *The Journal of Experimental Medicine,* vol. 41, no. 4, pp. 439-443, 1925.

[12] J. F. Danielli and H. Davson, "A contribution to the theory of permeability of thin films," *Journal of cellular and comparative physiology,* vol. 5, no. 4, pp. 495-508, 1935.

[13] S. J. Singer and G. L. Nicolson, "The fluid mosaic model of the structure of cell membranes," *Science,* vol. 175, no. 4023, pp. 720-731, 1972.

[14] O. G. Mouritsen and M. Bloom, "Mattress model of lipid-protein interactions in membranes," *Biophys. J.,* vol. 46, pp. 141-153, 1984.

[15] T. Heimburg, Thermal biophysics of membranes, Wiley-VCH, 2007.

[16] S. Chandrasekhar, Liquid Crystals, Second ed., Cambridge University Press, 1992.

[17] T. Hainik, “Structure and physical properties of biomembranes and model membranes,” *Acta Physica Slovaca,* vol. 56, pp. 678-806, 2006.

[18] H. Ebel, P. Grabitz and T. Heimburg, “Enthalpy and volume changes in lipid membranes. I. The proportionality of heat and volume changes in the lipid melting transition and its implication for the elastic constants,” *J. Phys. Chem. B.,* vol. 105, pp. 7353-7360, 2001.

[19] I. P. Sugár, “A theory of the electric field-induced phase transition of phospholipid bilayers,” *Biochimica et Biophysica Acta (BBA),* vol. 556, no. 1, pp. 72-85, 1979.

[20] R. M. J. Cotterill, “Field effects on lipid membrane melting,” *Physica Scripta,* vol. 18, no. 3, p. 191, 1978.

[21] D. Johnston and S. M. S. Wu, Cellular Neurophysiology, Boston, Massachusetts: MIT Press, 1995.

[22] K. Iwasa, I. Tasaki and R. C. Gibbons, “Swelling of nerve fibres associated with action potentials,” *Science,* vol. 210, pp. 338-339, 1980.

[23] K. Iwasa, I. Tasaki and R. C. Gibbons, “Mechanical changes in crab nerve fibers during action potentials,” *Jpn. J. Physiol.,* vol. 30, pp. 897-905, 1980.

[24] W. Carius, “Voltage dependence of bilayer membrane capacitance,” *J. Coll. Interf. Sci.,* vol. 57, pp. 301-307, 1976.

[25] K. Vanselow, “Studies on the electrostatic-mechanical forces of the nerve membrane upon stimulation of the action potential,” *Z. Dt. Gesellsch. Med. Biol. Elektronik,* vol. 11, pp. 1-5, 1966.

[26] Sigma-Aldrich Co. LLC, “Oleic acid,” [Online]. Available: http://www.sigmaaldrich.com/catalog/product/sial/o1008?lang=en&region=DK.

[27] “Dielectric materials,” University of Cambridge, [Online]. Available: http://www.doitpoms.ac.uk/tlplib/dielectrics/index.php.

[28] “Effect of structure on the dielectric constant,” University of Cambridge, [Online]. Available: http://www.doitpoms.ac.uk/tlplib/dielectrics/structure.php.

[29] “Relative Dielectric Constants,” ifm electronic ltd. - United Kingdom, [Online]. Available: http://www.ifm.com/img/dialectric_constants.pdf.

[30] K. Zecchi, “Master's Thesis Electro-mechanical properties of lipid membranes at their phase transitions,” Copenhagen University, Niels Bohr Insitute, 2013.

[31] F. F. d. Sousa, P. T. C. Friere, J. M. Filho, A. C. Oliveira, P. H. M. d. Vasconcelos, G. D. Saraiva, S. G. C. Moreira and P. Alcantara Jr., “Efect of impurities on the dielectric properties of oleic acid,”

*Journal of Advanced Dielectrics,* vol. 2, no. 3, pp. 1-8, 2012.

[32] R. M. J. Cotterill, “Field effects on lipid membrane melting,” *Physica Scripta,* vol. 18, no. 3, p. 191, 1978.

[33] F. F. d. Sousa, J. Del Nero, S. G. C. M. Moreira, S. J. d. S. d. Silva and P. Alcantara Jr., “Dielectric Properties of Oleic Acid in Liquid Phase,” *Journal of Bionanoscience,* vol. 3, pp. 1-4, 2010.

[34] A. Garcia-Quiroz, S. G. C. Moreira, A. V. de Morais, A. S. Silva, G. N. da Rocha and P. Alcantara, “Physical and Chemical Analysis of Dielectric Properties and Differential Scanning Calorimetry Techniques on Buriti Oil,” *Instrumentation Science & Technology,* vol. 31, no. 1, pp. 93-101, 2003.

[35] R. A. Freedman and H. D. Young, University Physics, San Francisco: Pearson Addison-Wesley, 2008.

[36] “Vegetable Oil Fatty Acid Composition,” The Paleo Diet, [Online]. Available: http://thepaleodiet.com/vegetable-oil-fatty-acid-composition/.

[37] “Metals and Alloys - Densities,” The Engineering ToolBox, [Online]. Available: http://www.engineeringtoolbox.com/metal-alloys-densities-d_50.html.

# Appendix

### Theoretical calibration for thermal expansion

All materials have a thermal expansion coefficient which describes, for a given mass, a material's change in volume, planar area or one of the orthogonal lengths, in response to a change in its temperature. The linear, area and volumetric coefficients of thermal expansion at constant pressure are, respectively, defined as

$$\alpha_L = \frac{1}{L}\left(\frac{\partial L}{\partial T}\right)_P, \qquad \alpha_A = \frac{1}{A}\left(\frac{\partial A}{\partial T}\right)_P, \qquad \alpha_V = \frac{1}{V}\left(\frac{\partial V}{\partial T}\right)_P$$

where $L$ is length, $A$ is area, $V$ is volume, $\alpha_L$, $\alpha_A$, $\alpha_V$ are their corresponding coefficients of thermal expansion, and $T$ is temperature, at constant pressure.

The capacitor plates are made of copper and in all of the following we will assume that they are isotropic. The capacitor plates are planar cylinders with radius $r = 3.25$ cm and each plate has a width $W = 0.39$ cm. When the capacitor plates change dimensions with temperature, we are interested in how much the plate surfaces move toward one another and how much their planar area changes. Thus the thermal expansion area of interest, namely where charge accumulates during measurements, is the effective capacitor area

$$A_0 = A_{eff} = 31.98\text{cm}^2$$

The theoretical area is $A_{theoretical} = \pi r^2 = \pi(3.25\text{cm})^2 = 33.18\text{cm}^2$, we can determine the effective radius

$$r_{eff} = 3.19\text{cm}$$

and with the assumption that the capacitor plates are isotropic, we can now define the thermal length of expansion of interest as the effective half width distances from the planar centres of the plates:

$$L_0 = L_{eff} = 2 \cdot \frac{W_{eff}}{2} = W = 0.39\text{cm}$$

The linear thermal expansion coefficient of copper at 20°C is $\alpha_{L,c} = 1.7 \cdot 10^{-5}\ \text{K}^{-1}$ [35]. It is positive and we will assume that for the temperature range $0°\text{C} \leq T \leq 40°\text{C}$ of the experiments, it is constant[6]. The area expansion coefficient for copper could not be found anywhere, but it can be calculated as follows:

$$A = \pi r^2$$

$$dA = \frac{dA}{dr} dr = 2\pi r\, dr$$

[6] Though for most materials the thermal expansion coefficient is temperature dependent, and not always linear, no information can be found with respect this for copper.

Since,

$$dr = \alpha_r \cdot r_0 \cdot dT$$

and

$$A_0 = \pi r_0^2 \,,$$

then

$$dA = 2\pi r_0 \cdot \alpha_r r_0 dT = 2\pi r_0^2 \alpha_r dT = 2\alpha_r A_0 dT$$

Isotropy implies $\alpha_r = \alpha_L$, therefore

$$dA = 2\alpha_L A_0 dT$$

So the thermal area expansion coefficient for copper is

$$\alpha_{A,c} = 2\alpha_{L,c} = 3.4 \cdot 10^{-5}\ \mathrm{K}^{-1}$$

For our capacitor,

$$\delta A = A_0 \alpha_{A,c}\, dT$$

$$\delta d = L_0 \alpha_{L,c} dT$$

where we, for simplicity, redefine $A_0$ and $L_0$ as the initial effective area and initial effective length at $T = 0$°C (273K), assuming that $A_{eff}$is the effective area at 20°C:

$$A_0 = A_{eff}\left(1 + \alpha_{A,c} dT\right) = 31.98\mathrm{cm}^2 \cdot \left(1 + \left(3.4 \cdot 10^{-5} \cdot (-20\ \mathrm{K})\right)\right) = 31.96\mathrm{cm}^2$$

$$L_o = L_{eff}\left(1 + \alpha_{L,c} dT\right) = 0.39\mathrm{cm} \cdot \left(1 + \left(1.7 \cdot 10^{-5} \cdot (-20\ \mathrm{K})\right)\right) = 0.3898708\mathrm{cm}$$

There seems to be very little difference between the effective values at room temperature and the new values and the corresponding $\delta A$ and $\delta L$ in the above calculation are -0.02cm$^2$ and $-1.292 \cdot 10^{-4}\mathrm{cm} = -1.292\mu\mathrm{m}$. Since the change in area is very small compared to the total area, it is disregarded in the analysis in Figure 17.